

Ab Initio Study of the Spectroscopy of $(\text{CH}_3)_3\text{CN}$ and $(\text{CH}_3)_2\text{CHN}$

Chun-Yuan Hou, Qing-Chuan Zheng, Zeng-Xia Zhao, and Hong-Xing Zhang*

State Key Laboratory of Theoretical and Computational Chemistry, Institute of Theoretical Chemistry Jilin University, Changchun, 130023, China

Received: March 13, 2007; In Final Form: August 13, 2007

Using the complete active space self-consistent field (CASSCF) method with 6-311++g(3df,3pd) basis sets, a few electronic states of nitrenes $(\text{CH}_3)_3\text{CN}$ and $(\text{CH}_3)_2\text{CHN}$ and their positive ions are calculated. All calculated states are valence states, and their characteristics are discussed in detail. In order to investigate the Jahn–Teller effect on $(\text{CH}_3)_3\text{CN}$ radical, C_s symmetry was used for $(\text{CH}_3)_3\text{CN}$ and $(\text{CH}_3)_2\text{CHN}$ in the calculations. The results of our calculations (CASPT2 adiabatic excitation energies and RASSI oscillator strengths) suggest that the calculated transitions of $(\text{CH}_3)_3\text{CN}$ at 27 710 cm^{-1} and $(\text{CH}_3)_2\text{CHN}$ at 28 110 cm^{-1} are attributed to $2^3A'' \rightarrow 1^3A''$, while those of $(\text{CH}_3)_3\text{CN}$ at 28 916 cm^{-1} and $(\text{CH}_3)_2\text{CHN}$ at 29 316 cm^{-1} are attributed to $1^3A' \rightarrow 1^3A''$. The vertical and adiabatic ionization energies were obtained to compare with the photoelectron spectroscopic data. These results are in agreement with previous experimental data. Also, we present a comprehensive review on the CAS calculation results for $(\text{CH}_3)_n\text{CH}_{3-n}\text{N}$ ($n = 0-3$) presented in our previous and present papers.

I. Introduction

Nitrenes (molecules formulated as R–N) contain electron-deficient nitrogen atoms¹ and have received increasing attention in experimental and theoretical studies in recent years, not only because the nitrenes are short-lived intermediates in many organic and inorganic reactions,^{2,3} but also because of the small energy separation between their lowest single and triplet states. The most thoroughly studied nitrenes are amidogen, NH, and phenylnitrene, $\text{C}_6\text{H}_5\text{N}$.⁴⁻⁷ A few experimental and theoretical studies have been reported on the excitation spectroscopy and photoelectron spectroscopy of CH_3N and $\text{CH}_3\text{CH}_2\text{N}$;⁸⁻¹⁹ however, much less is known about $(\text{CH}_3)_3\text{CN}$ and $(\text{CH}_3)_2\text{CHN}$.

Several studies by photoelectron spectroscopy (PES) were carried out that were mainly concerned with the vertical ionization of different molecular orbitals of $(\text{CH}_3)_2\text{CHN}$.²⁰ Wang et al. reported four experimental energies in the low ionization energy region for $(\text{CH}_3)_2\text{CHN}$. They also performed some limited ab initio calculations of the vertical ionization energies according to C_s symmetry from the G2 and DFT methods to explain their findings for $(\text{CH}_3)_2\text{CHN}$. However, the structures and properties of the ground and excited states that would be of importance in the neutral compounds and their cations ($(\text{CH}_3)_3\text{CN}^+$ and $(\text{CH}_3)_2\text{CHN}^+$) were not treated and need to be further investigated. Moreover, besides the vertical ionization energies they calculated, adiabatic energies with geometric relaxation of the excited state would be an important contribution to the ionization energies and to explain the characteristics of the electronic states.

To the best of our knowledge, there are no reported theoretical studies on the excitation spectroscopy of $(\text{CH}_3)_3\text{CN}$ and $(\text{CH}_3)_2\text{CHN}$, although a few experimental and theoretical studies were reported on the pyrolysis of nitrenes such as CH_3N , $\text{CH}_3\text{CH}_2\text{N}$, $(\text{CH}_3)_2\text{CHN}$, and $(\text{CH}_3)_3\text{CN}$.²¹ It is best known that the CASSCF (complete active space self-consistent field) and CASPT2

(multiconfiguration second-order perturbation theory) methods are effective for theoretical studies of excited electronic states of molecules and molecular ions.^{22,24} By using the CASSCF and CASPT2 methods, we previously studied and characterized a large number of electronic states of CH_3N and $\text{CH}_3\text{CH}_2\text{N}$ and their ions.⁸ The aim of the present paper is to study and characterize a large number of electronic states of $(\text{CH}_3)_3\text{CN}$ and $(\text{CH}_3)_2\text{CHN}$ and their positive ions. Equilibrium geometries, adiabatic excitation energies, and oscillator strengths for the low-lying states of neutral compounds and their positive ions at the CASPT2//CASSCF level of theory that give insight into the characteristics of the electronic states are determined. Preliminary results are also obtained for the vertical and adiabatic ionization energies of different orbitals of C_s symmetry for $(\text{CH}_3)_3\text{N}$ and $(\text{CH}_3)_2\text{CHN}$, and they are in agreement with experimental data. In the conclusion of the present article, we will compare the calculation results for $(\text{CH}_3)_3\text{N}$ and $(\text{CH}_3)_2\text{CHN}$ with those for CH_3N and $\text{CH}_3\text{CH}_2\text{N}$.⁸

II. Methodology

Choice of the active space is the essential step in the calculations with the CASSCF method. For $(\text{CH}_3)_2\text{CHN}$ and $(\text{CH}_3)_3\text{CN}$, the CH_3 group is stable. To keep a balance between the computation cost and the computation precision, we chose eight electrons activated in 15 molecular orbitals, which means 9 a' orbitals and 6 a'' orbitals for $(\text{CH}_3)_2\text{CHN}$, and we chose eight electrons activated in 18 molecular orbitals, which means 11 a' orbitals and 7 a'' orbitals for $(\text{CH}_3)_3\text{CN}$. The geometry of every state was optimized at the CASSCF level of theory. Second-order perturbation (CASPT2) was used to consider the dynamic correction. According to the CASPT2 energies calculated at the respective geometries optimized at the CASSCF level, we obtained the CASPT2//CASSCF adiabatic excitation energy values.

For all of the calculations we employed extended basis sets, denoted as 6-311++g(3df,3pd) basis, which contain polarization and diffuse basis functions to give sufficient flexibility to

* To whom correspondence should be addressed. E-mail: zhanghx@mail.jlu.edu.cn.

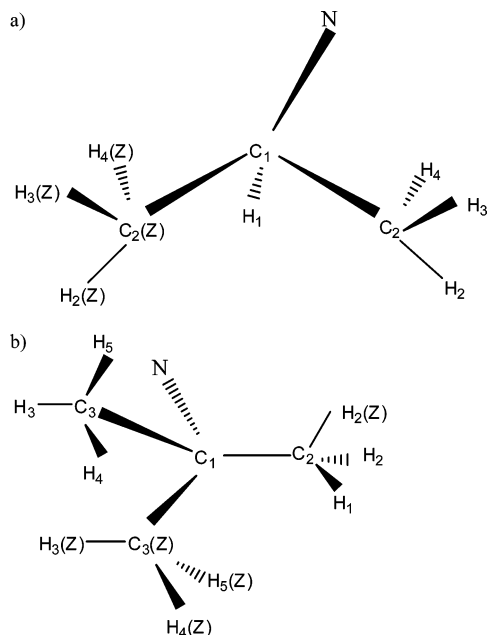


Figure 1. Molecular geometries of (a) $(\text{CH}_3)_2\text{CHCN}$ and (b) $(\text{CH}_3)_3\text{CN}$.

describe a variety of electronic states. The same basis sets were employed in our previous study on CH_3N and $\text{CH}_3\text{CH}_2\text{N}$. That the $d_{x^2+y^2+z^2}$ type basis is treated as an s-type basis is the reason for excess electrons in the s orbitals in the Mulliken population analysis in some cases. It gives the contraction scheme (12s,-6p,3d,1f)/[5s,4p,3d,1f] for N and C atoms and (6s,3p,1d)/[4s,-3p,1d] for H atom with a total of 282/357 contractions for $(\text{CH}_3)_2\text{CHN}/(\text{CH}_3)_3\text{N}$ and their positive ions.

The oscillator strength is defined as

$$f = 2(\text{TDM})^2 \Delta E / 3$$

The transition moments (TDM) were computed by CASSCF, and the excitation energies, which are very sensitive to dynamic correlation, were computed by CASPT2.²⁴

The molecular geometries of $(\text{CH}_3)_2\text{CHN}$ and $(\text{CH}_3)_3\text{CN}$ are shown in Figure 1. The optimized geometry of the ground state of $(\text{CH}_3)_3\text{CN}/(\text{CH}_3)_2\text{CHN}$ was used to calculate the vertical ionization energies, which are obtained from the difference of the total energies between the resulting radical ion and the neutral $(\text{CH}_3)_3\text{CN}/(\text{CH}_3)_2\text{CHN}$ radical. The calculated adiabatic ionization energies are obtained from the difference of the total energies between the radical ion and the neutral $(\text{CH}_3)_3\text{CN}/(\text{CH}_3)_2\text{CHN}$ radical in their respective optimized geometries. All the CAS calculations were performed using the MOLCAS 6.0 quantum-chemistry software²⁵ on a Lenovo/1800 server.

III. Results and Discussion

A. Adiabatic and Vertical Excitation Energies and State Characteristics of $(\text{CH}_3)_3\text{CN}$ and $(\text{CH}_3)_2\text{CHN}$. The calculation of the excitation spectrum is a natural starting point for a thorough investigation of the excited states of any polyatomic system. A few electronic states are calculated by the CASSCF method, which provides us with dipole transition moments for the calculation of oscillator strengths. Furthermore, the configuration interaction (CI) vectors of the CASSCF wave function give insight into the structure of the respective electronic state and will be discussed in the following. For all the calculated states, the accuracy of the adiabatic excitation energies was

improved by including dynamic electron correlation by the CASPT2 method.

1. CASPT2//CASSCF Results for the Ground and Excited States of $(\text{CH}_3)_2\text{CHN}$ and $(\text{CH}_3)_3\text{CN}$. Equilibrium structures of the ground states and 5/7 lowest excited states of $(\text{CH}_3)_3\text{CN}/(\text{CH}_3)_2\text{CHN}$ by CASSCF were optimized to obtain good starting guesses and approximate Hessians for the computationally extremely demanding CI optimizations. The equilibrium geometries of all the states with C_s symmetry are obtained at the CASPT2//CASSCF level and are summarized in Tables 1 and 2, which also contain energies and oscillator strengths.

Hyperconjugation arguments are often evoked when discussing the bonding in open-shell systems, usually in the context of explaining ESR or PES data. In our calculations of $(\text{CH}_3)_3\text{CN}$, we find that the effect of $C_1\text{-N}$ hyperconjugation shortens the N-C_1 bond length, as shown in Figure 2c. Moreover, increased s character along the $C_1\text{-N}$ axis, characteristic of a strong σ -type N-C_1 bond, enhances the $C_1\text{-N}$ bonding interaction since excess electrons occupied the stabilized N-C_1 σ -type bond and is at the expense of s character in the $C_1\text{-C}_2$ bonds, which results in carbon p-type orbitals that play a more important role in the $C_1\text{-C}_2$ bonds. Thus it weakened $C_1\text{-C}_2$ bonds and made the $C_2\text{-C}_1\text{-C}_3$ bond angle tend to 90° , exactly as found in the optimized ground geometry. In the $2^3A''$ and $1^3A'$ excited states the σ -type N-C_1 bond is weakened because an electron transferred from the $C_1\text{-N}$ σ -type bond to the HOMO(2e) orbital, and the $C_1\text{-C}_2$ bonds are strengthened. Thus the $C_1\text{-N}$ bond is lengthened, the $C_2\text{-C}_1\text{-C}_3$ and $C_3\text{-C}_1\text{-C}_3(\text{X})$ bond angles are a little bigger, and the $\text{N-C}_1\text{-C}_2$ and $\text{N-C}_1\text{-C}_3$ bond angles are a little smaller.

The Jahn-Teller effect is evident in the ground state compared with our previous calculations on CH_3N ,⁸ because it distorts a little from C_{3v} symmetry. In the $3A'$ and $2^3A''$ excited states the geometry was distorted from C_{3v} symmetry a little as found throughout Table 1, since the $C_1\text{-N}$ is not bonding. The $C_1\text{-N}$ bond lengths in the $3A'$ and $2^3A''$ states are longer than the $C_1\text{-N}$ bond length in the $3A''$ state since an electron transferred from the σ -type N-C_1 bond.

The oscillator strengths for the transitions between the ground and excited states were calculated. To obtain a nonvanishing transition dipole moment, $\langle \psi_i | \hat{\mu} | \psi_j \rangle$, the direct product $\Gamma_i \times \Gamma_\mu \times \Gamma_j$ must contain the totally symmetric irreducible representation. In the case of the C_s point group, Γ_{μ_y} and Γ_{μ_z} are A' and the ground state symmetry is $1^3A''$; thus transitions into states of A'' symmetry are dipole allowed. Γ_{μ_x} is A'' and thus transitions into states of A' symmetry are dipole allowed. Our calculated oscillator strengths (cf. Table 1) reflect exactly these selection rules, and within numerical accuracy oscillator strengths of transitions into states $1A'$ and $1A''$ are above 10 orders of magnitude smaller than for $1^3A'$ and $2^3A''$. This also shows that transitions from triplet state into triplet states are available.

As shown in the Supporting Information, Table 5a gives the Mulliken population analysis for the $3A''$ ground state and the $1^3A'$ and $2^3A''$ excited states of $(\text{CH}_3)_3\text{CN}$. We can see that only the population on the C_1 and N atoms is different. In the ground state, the electronic configuration of the C_1/N atoms are $s^{3.410} p_x^{0.944} p_y^{0.643} p_z^{0.988} / s^{4.174} p_x^{1.024} p_y^{1.305} p_z^{1.030}$, while in the $2^3A''$ and $1^3A'$ excited states the configurations are $s^{3.537} p_x^{0.926} p_y^{0.460} p_z^{0.922} / s^{3.961} p_x^{1.911} p_y^{0.721} p_z^{0.981}$ and $s^{3.549} p_x^{0.895} p_y^{0.479} p_z^{0.932} / s^{3.944} p_x^{0.977} p_y^{0.715} p_z^{1.916}$, respectively. In the $2^3A'' \rightarrow 1^3A''$ and $1^3A' \rightarrow 1^3A''$ transitions at $27\,710\text{ cm}^{-1}$ and $28\,110\text{ cm}^{-1}$ about 0.89 p_x or p_y electron on the N atom is transferred to the s and p orbitals of C_1 and N atoms at the ratio 1:7 statistically. We

TABLE 1: Optimized Geometries, Leading Configurations, Occupation, and Respective Weights in the CI Vector (c^2), Excited Energies, and Oscillator Strengths of $(\text{CH}_3)_3\text{CN}$ and $(\text{CH}_3)_3\text{CN}^+$ Electronic States at C_s Symmetry at the CASPT2//CASSCF Level of Theory Using 6-311++g(3df,3pd) Basis Sets^a

state	R1 (Å)	R2 (Å)	R3 (Å)	$\alpha 1$ (deg)	$\alpha 2$ (deg)	$\alpha 3$ (deg)	$\alpha 4$ (deg)	occupation	weight	CASSCF E (au)	CASPT2 E (au)	T_0 (cm ⁻¹)	f
$(\text{CH}_3)_3\text{CN}$													
³ A''	1.438	1.529	1.559	109.8	107.4	111.2	109.8	(12a') ² (13a') ² (14a') ^u (6a'') ² (7a'') ^u	0.925	-211.315 624	-212.146 249		
¹ A'	1.434	1.531	1.550	112.3	106.4	111.2	109.2	(12a') ² (13a') ² (14a') ² (6a'') ² (7a'') ⁰	0.686	-211.277 491	-212.096 852	10 841	<10 ⁻¹⁰
								(12a') ² (13a') ² (14a') ⁰ (6a'') ² (7a'') ²	0.242				
¹ A''	1.401	1.573	1.547	107.6	109.6	109.9	110.0	(12a') ² (13a') ² (14a') ^u (6a'') ² (7a'') ^d	0.933	-211.254 064	-212.094 994	11 248	<10 ⁻¹⁰
² ¹ A'	1.438	1.535	1.549	108.7	108.4	110.8	109.6	(12a') ² (13a') ² (14a') ² (6a'') ² (7a'') ⁰	0.388	-211.237 021	-212.063 796	18 094	<10 ⁻¹⁰
								(12a') ² (13a') ² (14a') ⁰ (6a'') ² (7a'') ²	0.515				
² ³ A''	1.643	1.513	1.519	107.1	103.8	113.8	113.4	(12a') ² (13a') ^u (14a') ² (6a'') ² (7a'') ^u	0.918	-211.201 695	-212.019979	27 710	0.004
³ A'	1.652	1.511	1.519	103.0	105.5	114.1	113.3	(12a') ² (13a') ^u (14a') ^u (6a'') ² (7a'') ²	0.918	-211.203 448	-212.018 156	28 110	0.002
$(\text{CH}_3)_3\text{CN}^+$													
² A'	1.316	1.527	1.626	117.3	101.2	114.8	105.7	(12a') ² (13a') ² (14a') ^u (6a'') ² (7a'') ⁰	0.952	-210.936 274	-211.795 095		

^aR1 is N-C₁ distance, R2 is C₁-C₂ distance, R3 is C₁-C₃ distance, $\alpha 1$ is N-C₁-C₂ angle, $\alpha 2$ is N-C₁-C₃ angle, $\alpha 3$ is C₂-C₁-C₃ angle, and $\alpha 4$ is C₃-C₁-C₃(X) angle. All states were optimized at the CASPT2//CASSCF level using 6-311++g(3df,3pd) basis sets. The occupation numbers represent the electronic numbers that occupied the active space. "u" represents a spin-up electron, and "d" represents a spin-down electron.

TABLE 2: Optimized Geometries, Leading Configurations, Occupation, and Respective Weights in the CI Vector (c^2), Excited Energies, and Oscillator Strengths of $(\text{CH}_3)_2\text{CHN}$ and $(\text{CH}_3)_2\text{CHN}^+$ Electronic States at C_s Symmetry at the CASPT2//CASSCF Level of Theory Using 6-311++g(3df,3pd) Basis Sets^a

state	R1 (Å)	R2 (Å)	R3 (Å)	R4 (Å)	R5 (Å)	R6 (Å)	$\alpha 1$ (deg)	$\alpha 2$ (deg)	$\alpha 3$ (deg)	$\alpha 4$ (deg)	$\alpha 5$ (deg)	$\alpha 6$ (deg)	$\alpha 7$ (deg)	$\alpha 8$ (deg)	$\alpha 9$ (deg)	$\alpha 10$ (deg)	occupation	weight	CASSCF E (au)	CASPT2 E (au)	T_0 (cm ⁻¹)	f
$(\text{CH}_3)_2\text{CNH}$																						
³ A''	1.438	1.084	1.557	1.082	1.082	1.082	109.4	108.3	111.5	109.1	109.6	110.6	110.4	108.8	108.8	108.7	(9a') ² (10a') ² (11a') ^u (7a'') ² (8a'') ^u	0.928	-172.248 290	-172.898 115		
¹ A'	1.409	1.105	1.543	1.083	1.081	1.082	111.8	104.4	111.6	108.4	109.9	110.6	110.2	108.8	108.7	108.6	(9a') ² (10a') ² (11a') ² (7a'') ² (8a'') ⁰	0.420	-172.188 695	-172.848 202	10 953	<10 ⁻¹⁰
																	(9a') ² (10a') ² (11a') ⁰ (7a'') ² (8a'') ²	0.516				
¹ A''	1.411	1.088	1.565	1.082	1.080	1.082	109.9	108.8	110.9	108.7	109.2	110.3	110.1	109.1	109.1	109.0	(9a') ² (10a') ² (11a') ^u (7a'') ² (8a'') ^d	0.934	-172.189 558	-172.845 656	11 512	<10 ⁻¹⁰
² ¹ A'	1.428	1.091	1.545	1.083	1.081	1.082	110.5	106.8	111.3	108.8	109.6	110.5	110.4	108.8	108.8	108.7	(9a') ² (10a') ² (11a') ² (7a'') ² (8a'') ⁰	0.398	-172.168 939	-172.812 926	18 694	<10 ⁻¹⁰
																	(9a') ² (10a') ² (11a') ⁰ (7a'') ² (8a'') ²	0.510				
² ³ A''	1.605	1.078	1.514	1.086	1.080	1.080	106.1	104.2	115.1	112.2	107.9	110.9	110.8	108.4	109.4	109.4	(9a') ² (10a') ^u (11a') ² (7a'') ² (8a'') ^u	0.922	-172.141 024	-172.766 354	28 916	0.012
³ A'	1.626	1.077	1.514	1.086	1.078	1.081	108.0	98.7	114.8	112.9	108.6	110.7	110.6	109.2	108.6	109.1	(9a') ² (10a') ^u (11a') ^u (7a'') ² (8a'') ²	0.923	-172.138 879	-172.764 531	29 316	0.003
² ¹ A''	1.774	1.074	1.503	1.088	1.079	1.079	103.8	99.0	117.3	114.8	107.7	111.1	110.9	108.4	109.1	109.6	(9a') ² (10a') ^u (11a') ^d (7a'') ² (8a'') ²	0.920	-172.094 982	-172.722 405	38 559	<10 ⁻¹⁰
³ ¹ A'	1.774	1.076	1.505	1.088	1.078	1.081	105.5	95.1	117.5	114.7	108.0	111.0	110.9	109.1	108.4	109.3	(9a') ² (10a') ^u (11a') ² (7a'') ² (8a'') ^d	0.924	-172.091 322	-172.720 768	38 918	<10 ⁻¹⁰
$(\text{CH}_3)_2\text{CNH}^+$																						
² A'	1.279	1.080	1.733	1.075	1.074	1.073	104.8	120.5	99.3	112.5	101.7	103.8	108.7	113.5	114.2	113.6	(9a') ² (10a') ² (11a') ^u (7a'') ² (8a'') ⁰	0.895	-171.922 018	-172.536 591		
⁴ A''	3.314	1.079	1.470	1.096	1.084	1.076	98.6	75.1	125.6	117.1	104.1	110.0	113.7	105.6	110.2	112.6	(9a') ² (10a') ^u (11a') ^u (7a'') ² (8a'') ^u	0.949	-171.895 810	-172.507 198	6 450	<10 ⁻¹⁰
⁴ A'	1.458	1.077	1.672	1.074	1.092	1.074	111.8	113.3	96.5	111.0	110.2	92.4	110.7	113.6	114.7	113.0	(9a') ² (10a') ² (11a') ^u (7a'') ^u (8a'') ^u	0.933	-171.829 236	-172.463 159	16 116	<10 ⁻¹⁰
² ¹ A'	1.447	1.079	1.678	1.074	1.090	1.074	112.0	113.0	97.0	111.0	109.7	93.7	110.3	113.0	113.5	114.5	(9a') ² (10a') ² (11a') ^u (7a'') ^u (8a'') ^u	0.690	-171.776 946	-172.417 214	26 199	0.001
																	(9a') ² (10a') ² (11a') ^u (7a'') ^u (8a'') ^d	0.187				

^aR1 is N₁-C₁ distance, R2 is C₁-H₁ distance, R3 is C₁-C₂ distance, R4 is C₂-H₂ distance, R5 is C₂-H₃ distance, R6 is C₂-H₄ distance, $\alpha 1$ is N₁-C₁-C₂ angle, $\alpha 2$ is N₁-C₁-H₁ angle, $\alpha 3$ is C₂-C₁-C₂(Z) angle, $\alpha 4$ is C₂-C₁-H₁ angle, $\alpha 5$ is C₁-C₂-H₂ angle, $\alpha 6$ is C₁-C₂-H₃ angle, $\alpha 7$ is C₁-C₂-H₄ angle, $\alpha 8$ is H₂-C₂-H₃ angle, $\alpha 9$ is H₂-C₂-H₄ angle, and $\alpha 10$ is H₃-C₂-H₄ angle. The occupation numbers represent the electronic numbers that occupied the active space. "u" represents a spin-up electron, and "d" represents a spin-down electron.

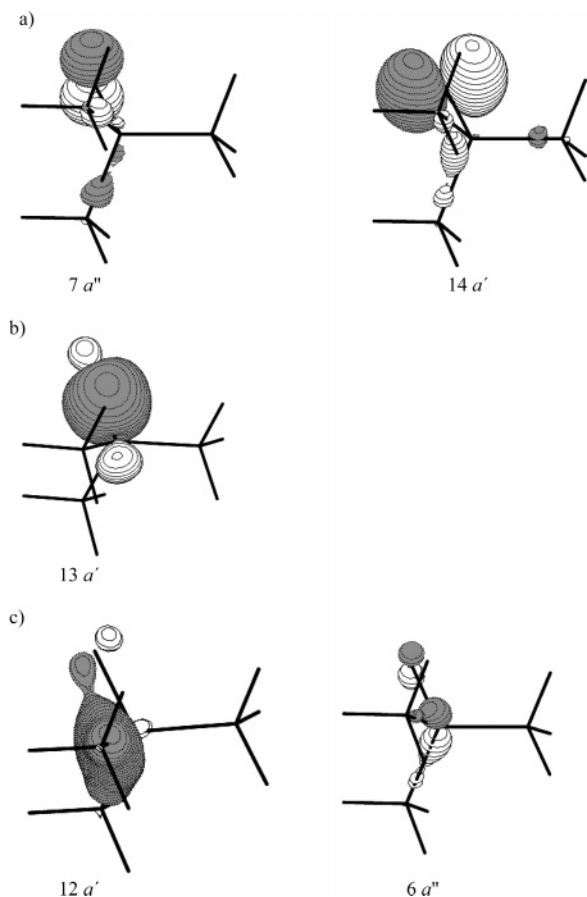


Figure 2. Selected molecular orbitals of the (a) $(ps)_n$, (b) $(sp)_\sigma$, and (c) $(pp)_\pi$ orbitals of $(CH_3)_3CN$ in the ground state at CASSCF optimized geometry.

assigned it to be $(ps)_n \rightarrow (sp)_\sigma$ in nature, which could be visually displayed by the corresponding density maps of molecular orbitals in Figure 2a,b. We can also see that in the $2^1A'$ state of $(CH_3)_3CN^+$ an electron definitely moves away from the $(ps)_n$ orbital. The evident change of population on C_2 or C_3 atoms compared to that in the $2^3A''$ and $1^3A'$ excited states of $(CH_3)_3CN$ is the reason for the shorter N– C_1 bond length, which strengthens the N– C_2 or N– C_3 interaction. We can see analogous results for $(CH_3)_2CNH$ in Table 5(b); however, the effect of hyperconjugation is more than that in $(CH_3)_3CN$ and the orbital character is a little different in the $2^3A''$ and $1^3A'$ excited states of $(CH_3)_2CNH$. Except for the two excited states of $(CH_3)_2CNH/(CH_3)_3CN$ in the $1^1A'$ and $1^1A''$ excited states at excitation energies of 10 953 and 11 512 cm^{-1} /10 841 and 11 248 cm^{-1} , respectively, excitation energies are all above the photodissociation limit of 17 000–18 000 cm^{-1} . However, there are no experimental reports on the $2^1A'$, $3^1A'$, or $2^1A''$ state. Perhaps more advanced spectroscopic techniques would be capable of observing these states, which might be an interesting challenge for experimentalists. The CASPT2//CASSCF adiabatic excitation energies (T_0) and state properties yield a picture of the electronic spectrum of $(CH_3)_3CN$ and $(CH_3)_2CNH$, including several states never calculated or measured before. The triplet/singlet splitting energies were calculated to be 1.344 and 1.358 eV for $(CH_3)_3CN$ and $(CH_3)_2CNH$, respectively.

The results for $(CH_3)_2CHN$ are summarized in Table 2. By comparing the results of $(CH_3)_2CHN$ with $(CH_3)_3CN$, we find the following: (1) In the ground state the N–C distance of $(CH_3)_2CHN$ is longer than that of $(CH_3)_3CN$ since the N–C bonding of $(CH_3)_2CHN$ is weaker than that of $(CH_3)_3CN$. In the $3^1A'$ and $2^3A''$ excited states the N–C bonds are weakened

TABLE 3: Calculated Vertical Ionization Energies (E_v), Adiabatic Ionization Energies (E_a), and ΔE ($E_v - E_a$) of $(CH_3)_2CNH$ and $(CH_3)_3CN$ According to C_s Symmetry from the CASPT2//CASSCF Method

cationic states	associated orbitals	E_v [ev]	E_a [ev]	ΔE (cm^{-1})	exptl ^a
$(CH_3)_2CNH$					
$2^1A'$	$6a''$	10.41	9.84	4597	9.70
$2^1A''$	$11a'$	10.61			10.72
$4^1A''$	$10a'$	11.25	10.64	4920	12.56
$4^1A'$	$5a''$	12.77	11.84	7500	
$(CH_3)_3CN$					
$2^1A'$	$7a''$	10.14	9.56	4678	
$2^1A''$	$14a'$	10.30			
$4^1A''$	$13a'$	10.93			
$4^1A'$	$6a''$	12.25			

^a Reference 20.

TABLE 4: Vertical Excitation Energies (T_v , in nm) for Low-Lying Excited Electronic States of $(CH_3)_3CN$ and $(CH_3)_2CNH$ Obtained in the CASPT2 Calculations with 6-311++g(3df,3pd) Basis Sets

	absorption (T_v)		emission (T_v)	
	$1^3A'' \rightarrow 1^3A'$	$1^3A'' \rightarrow 2^3A'$	$1^3A'' \leftarrow 1^3A'$	$1^3A'' \leftarrow 2^3A'$
$(CH_3)_3CN$	336	340	383	392
$(CH_3)_2CNH$	324	333	379	374

in $(CH_3)_2CHN$ and ruptured in $(CH_3)_3CN$. (2) The effect of hyperconjugation is strengthened by replacing a CH_3 group with a H atom. (3) The blue shift of the adiabatic excitation energies is due to the CH_3 group which delocalizes the electron between the N and C atoms (cf. Table 4). The vertical transition energies were also obtained for $(CH_3)_3CN$ and $(CH_3)_2CHN$ (cf. Table 4). All these results are analogous to our previous research on CH_3N and CH_3CH_2N .⁸

2. Characteristics of Electronic States. With the CASSCF framework, each state is characterized by its CI vector, which in general is easily interpreted. Most states can be well described by one dominant electron configuration that reveals the excitation process by which the respective state arises from the electronic ground states. In Tables 1 and 2, we compile the leading electron configurations, occupations, in which “u” represents that an electron spin orientation is up and “d” is down, and their respective weights (c^2) in the CASSCF wave function for all calculated states. The $(CH_3)_3CN$ ground state distorts a little from C_{3v} symmetry because of the Jahn–Teller effect and is predominantly $(12a')^2(6a'')^2(13a')^2(14a')^1(7a'')^1$, in which the energy difference between $12a'$ and $6a''$ orbitals or $14a'$ and $7a''$ orbitals is small as shown in Figure 2a,c. The $(CH_3)_2CHN$ ground state is predominantly $(9a')^2(7a'')^2(10a')^2(11a')^1(8a'')^1$. In the $(CH_3)_3CN$ ground state, the two unpaired electrons reside in the $14a'$ and $7a''$ molecular orbitals, which are perpendicular to the N–C bond and are mostly composed of the $2p_y$ and $2p_x$ orbitals of the N atom and show a small degree of the N– C_2 and N– C_3 interaction character. States $1^1A'$ and $2^1A'$ mainly result from single excitations between the two degenerate orbitals.

In fact, the majority of the calculated states arise from single or double excitations into the two orbitals which are the energetically lowest not completely occupied orbitals in the ground state. In the ground state of $(CH_3)_2CHN$, the two unpaired electrons reside in the $11a'$ and $8a''$ orbitals, between which the calculated orbital energy interval is small.

The c^2 values of all the states' leading configurations are above 0.9, indicating a single reference character of the respective states except for the $1^1A'$ and $2^1A'$ states of $(CH_3)_3-$

CN and (CH₃)₂CHN, which also reflect that the 14a' and 7a'' orbitals of (CH₃)₃CN in the ¹A' and ²1A' states are almost degenerate orbitals.

B. Excitation and Ionization Energies and State Characteristics of (CH₃)₃CN⁺ and (CH₃)₂CHN⁺. In order to further investigate the chemical properties of (CH₃)₃CN and (CH₃)₂-CHN, the ground and excited states of (CH₃)₃CN⁺ and (CH₃)₂-CHN⁺ were calculated by using the same basis sets and methods as the neutral molecules. All the states for the experimental C_s equilibrium geometry that were obtained at the CASPT2//CASSCF level are summarized in Tables 1 and 2, which contain energies and oscillator strengths. Furthermore, by using the optimized geometry of the ground state of (CH₃)₃CN/(CH₃)₂-CHN, the calculated vertical ionization energies were obtained from the difference of the total energies between the resulting radical ion and the neutral (CH₃)₃CN/(CH₃)₂CHN radical. The calculated adiabatic ionization energies were obtained from the difference of the total energies between the radical ion and the neutral (CH₃)₃CN/(CH₃)₂CHN radical in their respective optimized geometries.

1. *CASPT2//CASSCF Results for the Ground and Excited States of (CH₃)₃CN⁺ and (CH₃)₂CHN⁺.* The adiabatic excitation energies, which had never been reported, were calculated, and the results were summarized in Tables 1 and 2. The CASSCF calculations are not appropriate for a theoretical study of the ¹2A'' state of (CH₃)₃CN⁺ or (CH₃)₂CHN⁺ because there is no energy minimum unless it undergoes a pathway into their amine cations. However, even though the state exists, it is not the ground state of (CH₃)₃CN⁺ because the ¹2A' and ¹2A'' states in the ground state of (CH₃)₃CN⁺ in C_{3v} symmetry split due to Jahn–Teller effect and the ¹2A' state energy is lower than that in C_{3v} symmetry. We predict a weak transition in the adiabatic excitation spectrum of (CH₃)₂CHN⁺ at λ = 314 nm. In the ⁴A'' state of (CH₃)₂CHN⁺, it has the tendency to form its isomer, (CH₃)₂CNH⁺.

The c² values of the ²A', ⁴A'', and ⁴A'' state leading configurations of (CH₃)₂CH⁺ are above 0.89, indicating a single reference character of the respective states. In the ²2A' excited states the c² values of these states indicate a multireference character; we can predict in high excited states it will show high multireference character.

2. *Ionization Energies.* There have been some photoelectron spectroscopic experimental and theoretical reports about (CH₃)₂-CHN;¹⁸ however, their calculations were focused only on the vertical ionization energies. The adiabatic ionization energies and vertical ionization energies that are summarized in Table 3 were calculated, and that further proved their findings. The difference between the vertical and adiabatic ionization energies of (CH₃)₃CN is 0.58 eV. This means that the HOMO(2e) of the (CH₃)₃CN diradical is not nonbonding orbitals but has a small degree of the N–C2 and N–C3 interaction character, as described above.

IV. Conclusions

High-level ab initio calculations were performed in order to study and characterize some low-lying electronic states of (CH₃)₃CN and (CH₃)₂CHN and their positive ions using CASPT2//CASSCF methods with 6-311++g(3df,3pd) basis sets. In this section, we first briefly summarize the present work on (CH₃)₃CN and (CH₃)₂CHN and their positive ions and then present a comprehensive review on the CAS calculation results for (CH₃)_nCH_{3–n}N (n = 0–3) presented in our previous⁸ and present papers. In our previous⁸ paper, the CAS calculations were performed using the MOLCAS 5.4 program; to compare

the geometries and excitation energies, CASPT2//CASSCF calculations were also performed on the ¹3A'', ²3A'', and ¹3A' states of (CH₃)₃CN and (CH₃)₂CHN using the MOLCAS 5.4 program. The results are almost the same using the MOLCAS 5.4 and MOLCAS 6.0 programs.

The calculated transitions of (CH₃)₃CN at 27 710 and 28 111 cm⁻¹ are attributed to ²3A'' → ¹3A'' and ¹3A' → ¹3A'', respectively. They are assigned to be of (ps)_n → (sp)_σ in nature. For (CH₃)₂CHN the transition energy is blue shifted. In (CH₃)_nCH_{3–n}N (n = 0–3), the transition energy is red shifted since the CH₃ group delocalizes the electron between the N and C₁ atoms, and the oscillator strength is smaller as n increases. We predict a weak transition in the adiabatic excitation spectrum of (CH₃)₂CHN⁺ at λ = 314 nm.

We predict the geometries of several states of (CH₃)₃CN and (CH₃)₂CHN. Compared with our previous work on CH₃N and CH₃CH₂N, in (CH₃)_nCH_{3–n}N (n = 0–3), the N–C bond length is shorter as n increases in the ground state. The Jahn–Teller effect is greater on (CH₃)₃CN than on CH₃N.

Calculated ionization energies of (CH₃)₂CHN are compared with the experimental PES data. In (CH₃)_nCH_{3–n}N (n = 0–3), the first ionization energies are smaller as n increases, which is in good agreement with the experimental data.

Acknowledgment. This work is supported by the Natural Science Foundation of China (20573042, 20333050, 20173021).

Supporting Information Available: Tables of Mulliken charges. This material is available free of charge via the Internet at <http://pubs.acs.org>.

References and Notes

- Wentrup, C. *Reactive Molecules: The Neutral Reactive Intermediates in Organic Chemistry*; Wiley: New York, 1984; see Chapter 4.
- Sadygov, R. G.; Yarkony, D. R. *J. Chem. Phys.* **1997**, *107*, 4994.
- Kurosaki, Y.; Takayanagi, T.; Sato, K.; Tsunashima, S. *J. Phys. Chem. A* **1998**, *102*, 254.
- Cullin, D. W.; Lian, Y.; Williamson, J. M.; Platz, M. S.; Miller, T. A. *J. Phys. Chem.* **1990**, *94*, 3387.
- Huber, K.; Herzberg, G. *Constants of Diatomic Molecules*; Van Nostrand: New York, 1979.
- Baronovski, A. P.; Miller, P. G.; McDonald, J. R. *J. Chem. Phys.* **1978**, *30*, 119.
- Foy, B. R.; Casassa, M. P.; Stephenson, J. C.; King, D. S. *J. Chem. Phys.* **1989**, *90*, 7037.
- Hou, C. Y.; Zhang, H. X.; Sun, C. C. *J. Phys. Chem. A* **2006**, *110*, 10260.
- Carrick, P. G.; Engelking, P. C. *J. Chem. Phys.* **1984**, *81*, 1661.
- Chappell, E. L.; Engelking, P. C. *J. Chem. Phys.* **1988**, *89*, 6007.
- Ferrante, R. F. *J. Chem. Phys.* **1987**, *86*, 25.
- Carrick, P. G.; Brazier, C. R.; Bernath, P. F.; Engelking, P. C. *J. Am. Chem. Soc.* **1987**, *109*, 5100.
- Shang, H. R.; Yu, C.; Ying, L. M.; Zhao, X. S. *J. Chem. Phys.* **1995**, *103*, 4418.
- Shang, H. R.; Zhao, X. S. *Chem. Phys. Lett.* **1997**, *267*, 345.
- Demuyneck, J.; Fox, D.; Yamaguchi, J. Y.; Schaefer, H. F., III. *J. Am. Chem. Soc.* **1980**, *102*, 6204.
- Rechards, C.; Meredith, J. C.; Kim, S.; Quelch, G. E.; Schaefer, H. F., III. *J. Chem. Phys.* **1994**, *100*, 481.
- Ferrante, R. F.; Erickson, S. L.; Peek, B. M. *J. Chem. Phys.* **1987**, *87*, 2421.
- Wang, J.; Sun, Z.; Zhu, X. J.; Yang, X. J.; Ge, M. F.; Wang, D. X. *Angew. Chem., Int. Ed.* **2001**, *40*, 3055.
- Yang, X. J.; Sun, Z.; Ge, M. F.; Zheng, S. J.; Meng, L. P.; Wang, D. X. *ChemPhysChem* **2002**, *11*, 963.
- Sun, Z.; Wang, D.; Ding, R.; Ge, M. F.; Wang, D. X. *J. Chem. Phys.* **2003**, *119*, 293.
- Zeng, Y. L.; Sun, Q.; Meng, L. P.; Zheng, S. J.; Wang, D. X. *Chem. Phys. Lett.* **2004**, *390*, 362.
- Hou, X. J.; Huang, M. B. *Chem. Phys. Lett.* **2003**, *379*, 526.
- McLean, A. D.; Chandler, G. S. *J. Chem. Phys.* **1980**, *72*, 5639.
- Serrano-Andres, L.; Merchán, M.; Nebot-Gil, I.; Lindh, R.; Roos, B. O. *J. Chem. Phys.* **1993**, *98*, 3151.
- Andersson, K.; et al. *MOLCAS*, version 6.0; University of Lund: Sweden, 2004.